processes

MDPI

Article

Thermochemical Characteristics of Anaerobic Dairy Digestate and Its Pyrolysis Conversion for Producing Porous Carbon Materials

Chi-Hung Tsai [1,†], Hervan Marion Morgan, Jr. [2,†] and Wen-Tien Tsai [3,*]

[1] Department of Resources Engineering, National Cheng Kung University, Tainan 701, Taiwan; n48091089@gs.ncku.edu.tw
[2] Department of Tropical Agriculture and International Cooperation, National Pingtung University of Science and Technology, Neipu Township, Pingtung 912, Taiwan; p11222364@mail.npust.edu.tw
[3] Graduate Institute of Bioresources, National Pingtung University of Science and Technology, Pingtung 912, Taiwan
* Correspondence: wttsai@mail.npust.edu.tw; Tel.: +886-8-7703202
† These authors contributed equally to this work.

Abstract

In the present study, slurry digestate from a centralized anaerobic digestion (AD) plant, designed for dairy manure treatment and biogas-to-power generation, was utilized as a precursor for the preparation of porous biochars at elevated temperatures ranging from 550 to 850 °C. Proximate analysis and thermogravimetric analysis (TGA) were conducted to determine the thermochemical characteristics of the dried digestate and to explain its complex nature in relation to the physicochemical properties of the resulting biochars. Despite the substantial ash content of the precursor biowaste (approximately 30 wt%), primarily composed of inorganic compounds from calcium, the pore properties of the digestate-derived biochars had an overall increasing trend with regard to rising pyrolysis temperature. Nevertheless, some inconsistencies were observed between the samples produced at 550 °C and 850 °C, which highlighted the heterogeneous and complex nature of the precursor digestate. These observations can be attributed to active pyrolysis and the charring of the lignocellulosic components. The maximum Brunauer–Emmett–Teller (BET) surface area exceeded 200 m^2/g when pyrolysis was performed at 850 °C. Nitrogen (N_2) adsorption–desorption isotherms and scanning electron microscopy (SEM) confirmed that the porous digestate-based biochars predominantly exhibited both type I (microporous) and type IV (mesoporous) characteristics. Furthermore, the analytical results of energy-dispersive X-ray spectroscopy (EDS) and Fourier transform infrared spectroscopy (FTIR) indicated that oxygen-containing surface functional groups on the resulting biochars were retained after pyrolysis. The surface of the digestate-based biochar was also confirmed to be negatively charged at pH > 3.2.

Keywords: digestate; pyrolysis; biochar; pore property; chemical characteristics

check for updates

Academic Editors: Leandro Ayarde-Henríquez and Eduardo Chamorro

Received: 30 September 2025
Revised: 19 October 2025
Accepted: 20 October 2025
Published: 22 October 2025

Citation: Tsai, C.-H.; Morgan, H.M., Jr.; Tsai, W.-T. Thermochemical Characteristics of Anaerobic Dairy Digestate and Its Pyrolysis Conversion for Producing Porous Carbon Materials. *Processes* **2025**, *13*, 3380. https://doi.org/10.3390/pr13113380

Copyright: © 2025 by the authors. Licensee MDPI, Basel, Switzerland. This article is an open access article distributed under the terms and conditions of the Creative Commons Attribution (CC BY) license (https://creativecommons.org/licenses/by/4.0/).

1. Introduction

Livestock manure management has attracted global attention due to its contribution to greenhouse gas (GHG) emissions, pollution of receiving water bodies, and environmental odor issues. In this regard, the anaerobic digestion (AD) process has been recognized as an efficient approach for managing animal biowaste, which can simultaneously generate biogas for power generation (or fuel use) and produce digestate for agricultural

applications such as biofertilizers [1,2]. It was reported that an estimated 10,000 tons of solid digestate will be annually generated from a biogas plant with an installed capacity of 500 kW [3]. Based on the principles of the circular economy, AD-to-biogas systems are capable of mitigating GHG emissions, reducing fossil fuel consumption, and decreasing the use of chemical fertilizers. Consequently, the valorization and development of added-value applications for residual digestate have been extensively reviewed in the recent literature [4–13]. Among the available valorization strategies, pyrolysis, a thermochemical process, offers significant benefits over conventional disposal methods (e.g., landfilling and incineration) by converting AD-derived digestate into valuable products, thus reducing environmental impacts, GHG emissions and water contamination. Therefore, the production of porous biochar materials through thermochemical processes has been identified as a promising option. One of the key motivations has been the potential to recycle biochar or digestate-derived biochar back into the AD process in order to enhance biogas generation [14–21].

Despite this potential, relatively few studies have investigated the production of biochar from dairy farm digestate for use as a carbon precursor [22–25]. Qian et al. reported on the production of digestate-based biochars at 400–600 °C with a 60 min residence time under a 40 °C/min heating rate, aimed at producing products for carbon dioxide (CO_2) capture; however, the resulting BET surface areas were limited (11–16 m^2/g). Wang et al. produced digestate-based biochars at 400–800 °C with a 120 min residence time under a 10 °C/min heating rate. They reported an increasing trend in pore properties in relation to temperature increase and achieved a maximum BET surface area of approximately 250 m^2/g at 800 °C. Basinas et al. examined the pore and chemical properties of digestate-derived biochars produced at 300–700 °C with 180 min residence time and a 10 °C/min heating rate. Their investigation found that although the BET surface area increased with temperature, the maximum value was only about 100 m^2/g. Zheng et al. performed pyrolysis at 250–650 °C with a 120 min residence time and a 5 °C/min heating rate, focusing on the temperature-dependent variations in chemical characteristics. Their results indicated a decrease in carbon content and a corresponding increase in ash content as the pyrolysis temperature increased.

Previous studies on pig farm digestate extended the pyrolysis temperature range from 300 to 900 °C and residence times to 30 to 120 min [26,27]. These studies reported a maximum BET surface area of approximately 110 m^2/g for biochar produced at higher pyrolysis temperatures (800 °C) and shorter residence times (30 min). The relatively limited pore development was attributed to the high ash content of the precursor, which contained inorganic minerals such as calcium (Ca), silicon (Si), magnesium (Mg), phosphorus (P), iron (Fe), and potassium (K). In the present study, digestate from a dairy farm AD plant was employed to produce porous biochars in a vertical tube furnace across a temperature range of 550–850 °C with a fixed residence time of 30 min. To examine the complexity of the precursor digestate, its thermochemical characteristics were first determined. Subsequently, the pore properties, as well as the textural and chemical characteristics of the digestate-derived biochars, were investigated using porosimetry, energy-dispersive X-ray spectroscopy (EDS), scanning electron microscopy (SEM), Fourier-transform infrared spectroscopy (FTIR), and zeta potential analysis. The resulting data were interpreted in relation to the charring mechanisms that occurred during the pyrolysis process.

2. Materials and Methods

2.1. Materials

The precursor (digestate) used for producing porous biochar materials was obtained from a centralized dairy manure treatment plant located in Liouying Township (Tainan City,

Taiwan). This anaerobic digestion (AD) center was established to treat livestock manure from 21 nearby dairy farms, with a combined herd size of approximately 3600 Holstein cows. The slurry biowaste (water content > 80 wt%) was initially subjected to liquid–solid separation. The solid fraction was subsequently dried in an air-circulation oven at approximately 100 °C. The dried granular sample was then stored in a desiccator or maintained in the air-circulation oven (Taiwan HIPOINT Co., Kaohsiung city, Taiwan) until used in thermochemical analyses and pyrolysis experiments.

2.2. Determinations for Thermochemical Properties of Digestate

The thermochemical properties of the digestate were determined due to their significant influence on the pore structure and chemical characteristics of the resulting biochar products. Owing to its residual lignocellulosic components and nutrient/mineral content (e.g., nitrogen, phosphorus, potassium) after anaerobic digestion [1], the digestate can be considered a complex biowaste. Proximate analysis (ash, volatile matter, and fixed carbon) of the dried digestate was performed in triplicate following the American Society for Testing and Materials (ASTM) standards (D-3172). The fixed carbon content was calculated by difference (100% minus the sum of volatile matter and ash contents). The calorific value was measured in triplicate using a precision electronic calorimeter (Model: CALORIMETER ASSY 6200; Parr Instrument Co., Moline, IL, USA). Thermal decomposition behavior was evaluated using a thermogravimetric analyzer (Model: TGA-51; Shimadzu Co., Tokyo, Japan). The sample was heated from room temperature (25 °C) to 1000 °C at various heating rates (5, 10, 15, and 20 °C/min) under a nitrogen flow of 50 cm^3/min. Thermogravimetric (TGA) and derivative thermogravimetry (DTG) curves were recorded to guide the selection of the pyrolysis temperature range for biochar production. The surface elemental composition of the dried digestate was preliminarily determined using energy-dispersive X-ray spectroscopy (EDS) (Model: X-stream-2, Oxford Instruments, Abingdon, UK). Potassium quantification was excluded from EDS analysis because the characteristic X-ray peaks of potassium (K) overlapped with those of carbon (C), making them indistinguishable. Oxygen-containing functional groups were identified using a Fourier-transform infrared spectrometer (FTIR) (Model: FT/IR-4600; JASCO Co., Tokyo, Japan). Prior to FTIR analysis, a small amount of the sample was mixed with infrared-grade potassium bromide (KBr) and pressed into a disc using a hydraulic press (PIKE Co., Madison, WI, USA).

2.3. Pyrolysis Experim Ents

Porous biochar materials were produced in a vertical fixed-bed furnace following procedures similar to those reported in previous studies [26,27]. The process parameters were selected based on TGA-DTG results, which indicated complete thermal decomposition above 500 °C. Pyrolysis experiments were carried out at temperatures ranging from 550 to 850 °C with 100 °C intervals, and a fixed residence time of 30 min [26]. To account for heterogeneity in the precursor digestate, duplicate biochar samples were produced under identical conditions. The biochar products were designated as BC-D-temperature-I/II, where "I/II" indicated duplicates produced under the same conditions. All biochar samples were stored in an air-circulation oven at approximately 105 °C to prevent moisture adsorption prior to characterization.

2.4. Determinations for Pore and Chemical Characteristics of Digestate-Based Biochar Products

Pore properties of the digestate-derived biochars were determined using an automated porosimetry system (Model: ASAP 2020; Micromeritics Co., Moline, IL, USA) to measure BET surface area, pore volume, and pore size distribution. Prior to analysis, all samples were degassed under vacuum (≤10 μmHg) at 250 °C for 10 h. BET surface area was calculated using the Brunauer–Emmett–Teller (BET) model, while micropore surface area and

micropore volume were determined using the t-method (Harkins & Jura equation). Mesopore size distribution was obtained using the Barrett–Joyner–Halenda (BJH) equation [28], based on nitrogen adsorption–desorption isotherms at −196 °C. Total pore volume was calculated from the adsorbed amount of N_2 at a relative pressure of ca. 0.995, divided by the density of liquid nitrogen at −196 °C (0.8064 g/cm^3). Furthermore, micropore size distribution for pores < 2 nm was further determined using the Horvath–Kawazoe (HK) method based on low-pressure regions of the N_2 isotherms (P/P_0: 0–0.00115).

Surface morphologies were examined using a scanning electron microscope (SEM) (Model: Hitachi S-3000N; Hitachi Co., Tokyo, Japan) operated at 15 kV, with samples pre-coated with a thin layer of gold. Surface elemental compositions and functional groups were further confirmed using EDS and FTIR, as described in Section 2.2. Zeta potential measurements were conducted for selected biochar samples using a Zetasizer Nano ZS90 analyzer (Malvern Instruments, Worcestershire, UK) across a pH range of 3–11 to assess surface charge characteristics.

3. Results and Discussion

3.1. Thermochemical Characteristics of Digestate

As noted above, anaerobic digestate has been considered a potential precursor for biochar production due to its substantial content of partially degraded lignocellulosic components, particularly lignin. The results of the proximate analysis and calorific value for the dried digestate were measured in triplicate and are presented in Table 1. The digestate exhibited a relatively high ash content (28.14 wt%), which was attributed to its inherent composition and to the fact that the material originated from the bottom of the AD tank. When compared with other lignocellulosic residues [29], the calorific value of the digestate (18.87 MJ/kg, dry basis) was of a medium level, which was higher than that of residues with very high ash content (e.g., rice husk) but similar to that of low-ash materials such as wood. The thermal decomposition behavior of the dried digestate is illustrated in Figure 1, which shows the TGA and DTG curves obtained at heating rates of 5, 10, 15, and 20 °C/min under an inert atmosphere. All curves displayed similar patterns, with the decomposition peaks shifting toward higher temperatures at faster heating rates. As reported for other lignocellulosic biomasses [29], a slight weight loss was observed up to approximately 150 °C, which may be attributed to the desorption of physically adsorbed and bound moisture. Subsequently, the decomposition of the lignocellulosic constituents, particularly hemicellulose, occurred over a wide temperature range (250–550 °C), which led to the devolatilization and the onset of charring of cellulose and lignin above 450 °C. At elevated pyrolysis temperatures, more extensive carbonization and charring were promoted, resulting in biochar products that had enhanced pore development [30]. The final residual mass at 900 °C remained at approximately 40 wt%, which was consistent with the high ash content reported in Table 1.

Table 1. Proximate analysis, elemental analysis and calorific value of digestate.

Property	Value
Proximate analysis [a,b]	
Ash (wt%)	28.03 ± 0.42
Volatile matter (wt%)	58.91 ± 056
Fixed carbon [c] (wt%)	13.06
Elemental analysis [b,d]	

Table 1. *Cont.*

Property	Value
Carbon (wt%)	40.93
Oxygen (wt%)	38.85
Calcium (wt%)	8.31
Phosphorus (wt%)	2.63
Silicon (wt%)	2.58
Aluminum (wt%)	1.89
Sulfur (wt%)	1.54
Iron (wt%)	1.17
Sodium (wt%)	0.81
Magnesium (wt%)	0.69
Chlorine (wt%)	0.60
Calorific value (MJ/kg) [a,b]	18.87 ± 0.25

[a] Mean ± standard deviation for three determinations. [b] The values were determined by a dry-base sample. [c] By difference. [d] Determined by Energy Dispersive Spectrometer (EDS).

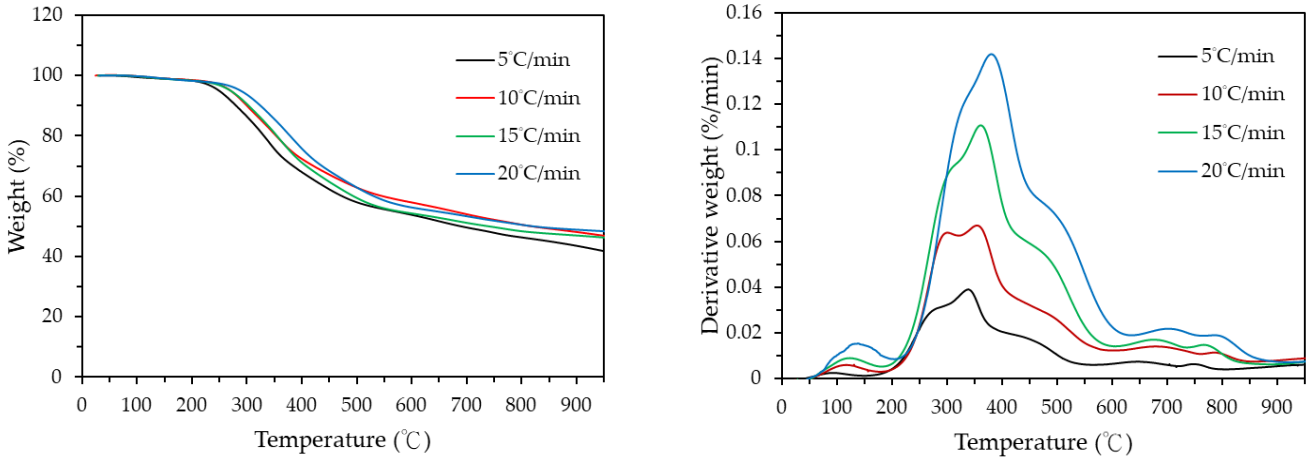

Figure 1. Curves of thermogravimetric analysis (TGA, (**left**) side) and derivative thermogravimetry (DTG, (**right**) side) for dried RH sample at various heating rates (i.e., 5, 10, 15 and 20 °C/min).

Table 1 also lists the preliminary values of elemental compositions for the dried digestate, revealing substantial amounts of carbon (40.93 wt%) and oxygen (38.85 wt%), along with notable concentrations of inorganic elements like calcium (8.31 wt%) and silicon (2.58 wt%). It should be noted that the diversified values and high ash content in Table 1 were related to the dairy feedstocks and digestion conditions. For example, the carbon content of anaerobic digestate will be reduced when extending the AD duration, leading to more carbon fractions being converted into methane. Thus, these results confirmed the heterogeneous and non-uniform nature of the digestate, despite its classification as a lignocellulosic biomass. The FTIR spectrum of the dried digestate, shown in Figure 2, confirmed the presence of various oxygen-containing functional groups on its surface [31–34]. The characteristic absorption bands at approximately 3440, 2920, 2350, 1650, and 1060 cm^{-1} were assigned to the stretching vibrations of O-H, C-H, conjugated C=C, C=O (or C=C stretch), and C-O functional groups, respectively.

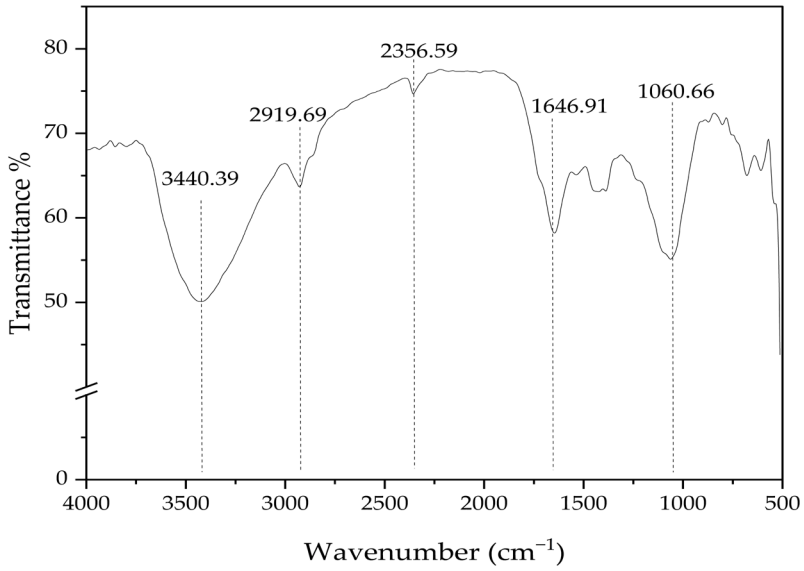

Figure 2. Fourier transform infrared spectroscopy (FTIR) spectra of dried digestate.

3.2. Pore Properties of Digestate-Based Biochar Products

Based on the N_2 adsorption–desorption isotherms at –196 °C, the pore characteristics of digestate-derived biochar products were determined and are summarized in Table 2. These data included the main pore parameters, including BET surface area, total pore volume, micropore surface area, micropore volume, and average pore diameter. To illustrate the pore structure, Figure 3 presents the N_2 adsorption–desorption isotherms for the optimal biochar product. Furthermore, Figures 4 and 5 also show the mesopore and micropore size distributions, respectively, based on the Barrett–Joyner–Halenda (BJH) and Horvath-Kawazoe (HK) methods [28]. The main findings derived from Table 2 and Figures 3–5 are summarized below:

1. As shown in Table 2, the pyrolysis temperature was a determining factor that influenced the pore properties of the digestate-based biochars. Biochar produced at 550 °C exhibited limited pore development, with a BET surface area of <20 m^2/g. By contrast, biochar produced at 850 °C showed a pronounced increase in pore properties, achieving the maximum values with a BET surface area greater than 190 m^2/g and a total pore volume exceeding 0.17 cm^3/g. These results suggested that pore development became more pronounced at higher pyrolysis temperatures due to enhanced charring [30,35], resulting in more developed porous structures. However, the BET surface areas of the biochars produced at 650 °C and 750 °C did not follow a consistent increasing trend compared with those produced at 550 °C and 850 °C, which reflected the heterogeneity and non-uniform nature of the digestate precursor. In addition, micropore properties (micropore surface area and micropore volume) were positively correlated with the total pore properties (BET surface area and total pore volume). Except for BC-D-550, the ratio of micropore contribution ranged from 60% to 70%, indicating that the resulting materials were predominantly microporous carbons. It should be noted that the calculated average pore diameters, which ranged from 1.7 nm to 4.0 nm, were not fully consistent with the microporous nature of the materials. This discrepancy could have arisen from the calculation assumption of independent cylindrical pores, whereas the actual pores in digestate-based biochars may have been slit-shaped and cross-connected.
2. According to the International Union of Pure and Applied Chemistry (IUPAC) classification of adsorption isotherms [36], microporous materials are typically associated with Type I isotherms, which exhibit high uptake in the low relative pressure re-

gion ($P/P_0 < 0.05$). Conversely, mesoporous materials are characterized by the Type IV isotherms, which display a hysteresis loop due to capillary condensation during adsorption and a different desorption mechanism. The initial part of the Type IV isotherm is generally attributed to monolayer-multilayer adsorption at relative pressures of about 0.40. The optimal digestate-based biochar (BC-D-850) displayed a combination of microporous and mesoporous characteristics, as evident from its isotherm profile (Figure 3). Moreover, the observed hysteresis loop corresponded to the IUPAC Type H4 classification, typically associated with narrow slit-shaped pores [28].

3. The pore size distributions derived from the BJH and HK methods are presented in Figures 4 and 5, respectively. As shown in Figure 4, a pronounced peak was observed at approximately 3.8 nm, indicating the presence of mesopores within the 2–50 nm range in the optimal biochar [28]. Additionally, significant microporosity within the 0.6–0.8 nm range was observed in Figure 5, consistent with the values reported in Table 2 and the isotherm profile in Figure 3.

Table 2. Pore properties of digestate-based biochar products.

Biochar (BC-D) Product [a]	S_{BET} [b] (m^2/g)	S_{micro} [c] (m^2/g)	V_t [d] (cm^3/g)	V_{micro} [e] (cm^3/g)	D_{ave} [f] (Å)
BC-D-550-I	15.44	2.41	0.0258	0.0007	62.09
BC-D-550-II	10.10	2.58	0.0069	0.0008	93.39
BC-D-650-I	90.76	61.63	0.0443	0.0266	33.16
BC-D-650-II	154.88	109.53	0.0678	0.0471	29.74
BC-D-750-I	121.44	84.39	0.0563	0.0362	31.80
BC-D-750-II	74.05	45.98	0.0706	0.0198	35.39
BC-D-850-I	209.44	115.30	0.1948	0.0496	36.46
BC-D-850-II	190.72	115.44	0.1630	0.4961	32.94

[a] Digestate-based biochar products (BC-D) were produced at 550–850 °C (by interval of 100 °C) under a fixed time of 30 min. [b] The Brunauer–Emmett–Teller (BET) surface area (S_{BET}) was calculated from the relative pressure (P/P_0) ranging from 0.05 to 0.150. [c] The micropore area was calculated from the *t*-plot method. [d] The total pore volume (V_t) was obtained at a relative pressure of about 0.995. [e] The micropore volume was calculated using the *t*-plot method. [f] The average pore diameter (D_{ave}) was estimated by the ratio of total pore volume (V_t) and BET surface area (S_{BET}), assuming that the pore is of cylindrical geometry (i.e., $D_{ave} = 4 \times V_t/S_{BET}$).

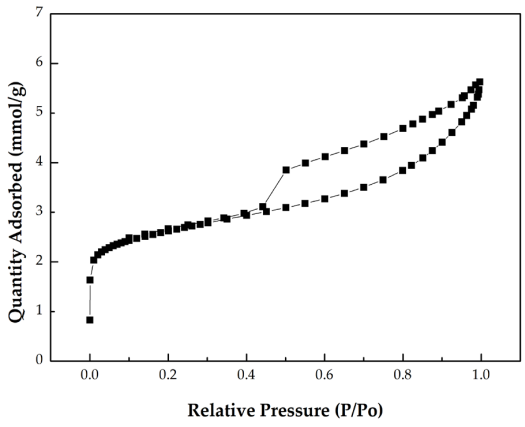

(**a**)

Figure 3. *Cont.*

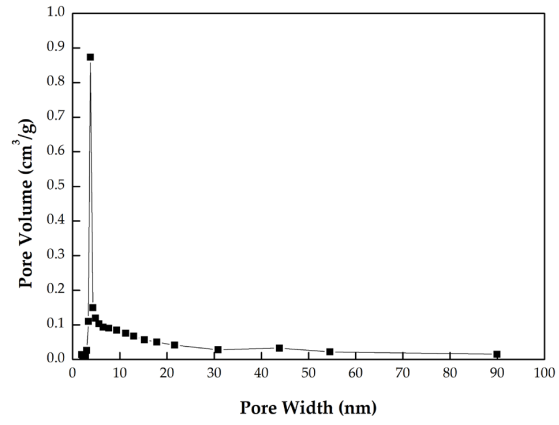

(**b**)

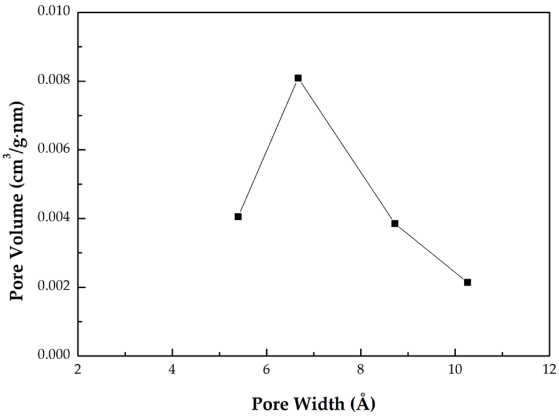

(**c**)

Figure 3. Pore characteristics of optimal biochar product (BC-D-850-I): (**a**) N2 adsorption–desorption isotherms; (**b**) mesopore size distribution; (**c**) micropore size distribution.

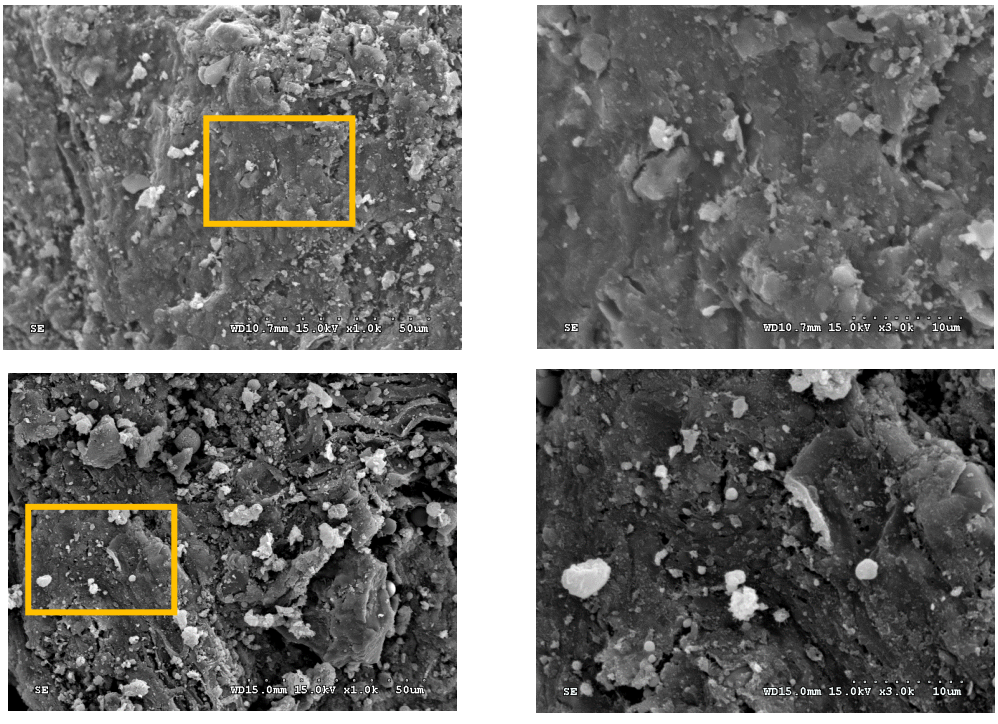

(**a**) (**b**)

Figure 4. SEM of (**a**) the biochar product (i.e., BC-D-550-I) and (**b**) the biochar product (i.e., BC-D-850-I).

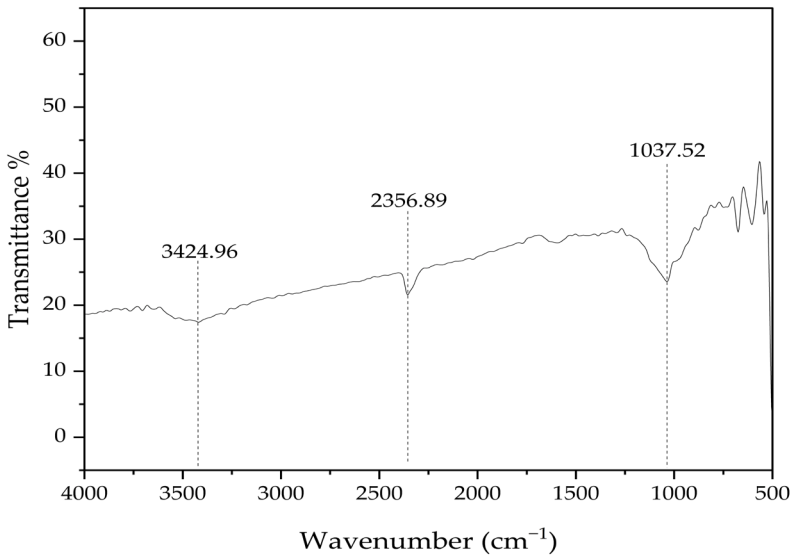

Figure 5. FTIR spectrum of optimal biochar product (i.e., BC-D-850-I).

3.3. Textural and Chemical Characteristics of Digestate-Based Biochar Products

As summarized in Table 2, the digestate-derived biochar products exhibited a porous structure. To visualize their microstructural features, scanning electron microscopy (SEM) was employed. Figure 4 presents the SEM images of two representative biochar products (BC-D-550-I and BC-D-850-I), which displayed markedly different pore properties, captured at magnifications of ×1000 and ×3000. The optimal biochar product (BC-D-850) appeared to possess a more irregular and complex surface morphology with a limited porous structure compared to BC-D-550. These observations were consistent with the property data reported in Table 2.

Elemental analysis was further conducted using energy-dispersive X-ray spectroscopy (EDS) to quantify the surface composition of the resulting biochars. Table 3 further lists the data on the elemental compositions of resulting digestate-based biochars produced at different pyrolysis temperatures. As expected, significant amounts of carbon and oxygen were detected on the biochar surfaces. Notably, BC-D-850 exhibited a markedly higher carbon content (52.95 wt%) and greater proportions of inorganic elements such as silicon (6.04 wt%) and aluminum (2.49 wt%), while showing reduced levels of oxygen (22.79 wt%) and calcium (7.58 wt%) compared with the precursor digestate as described in Table 1. On the other hand, the carbon contents of resulting digestate-based biochars were significantly lower than those (typically ranging from about 50 wt% to nearly 90 wt%) produced from other biomass-based biochars [37], reflecting that the anaerobic digestate contained high contents of inorganic elements.

The chemical functional groups were characterized using Fourier-transform infrared (FTIR) spectroscopy. Figure 5 presents the FTIR spectrum of BC-D-850-I. Compared with the precursor digestate, as shown in Figure 2, the peaks corresponding to oxygen-containing functional groups were significantly diminished or had disappeared, which suggested a reduction in surface oxygen due to thermal decomposition of lignocellulosic components and the release of pyrolytic gases (H_2O, CO, CO_2). As described in Section 3.1, the peak near 3425 cm^{-1} corresponded to the stretching vibration of hydroxyl (O-H) groups from adsorbed moisture. Peaks at approximately 2357 cm^{-1} and 1037 cm^{-1} were attributed to C=C (conjugated) and C-O (or C-O-C) groups in polysaccharides associated with aromatic or aliphatic structures [30–34]. Given the inherently high oxygen content of lignocellulosic biomass and its derived carbonaceous products (e.g., biochar), these materials are typically characterized by their polar and hydrophilic nature [38,39].

Table 3. Elemental compositions of resulting digestate-based biochars [1].

Elemental Composition	BC-D-550	BC-D-650	BC-D-750	BC-D-850
Carbon (wt%)	26.82	30.85	44.14	52.95
Oxygen (wt%)	36.71	36.32	31.46	22.79
Calcium (wt%)	19.00	9.06	6.82	7.58
Phosphorus (wt%)	5.71	4.07	4.56	1.17
Silicon (wt%)	2.98	9.09	5.25	6.04
Aluminum (wt%)	2.08	3.90	3.04	2.49
Other elements (wt%)	6.70	6.71	4.73	6.98

[1] Preliminarily determined by EDS analysis.

Surface charge properties were further evaluated by measuring zeta potential over a pH range of 3.0–11.0. Figure 6 shows the resulting zeta potential profile, which revealed that the surface of BC-D-850-I was positively charged at pH 3.0 but negatively charged across the higher pH range. By interpolating the zeta potential values between pH 3.0 and 5.0, the point of zero charge (pH_{zpc}) was estimated to be approximately 3.23. Accordingly, the surface of digestate-derived biochar was inferred to carry a net negative charge at pH values above this point, thereby enhancing its adsorption capacity for cationic species (e.g., heavy metal ions, methylene blue dye) through electrostatic attraction [39,40]. In contrast, the surface modifications of resulting digestate-based biochar material for enhancing the affinity of anionic (e.g., acid red 18 dye) or acidic species (e.g., CO_2) may be achieved by doping nitrogen-containing compounds (e.g., aniline) as the nitrogen atoms provide positive charges or binding sites [41,42]. When reusing the digestate-based biochar as an adsorbent, it may be deashed to enhance its adsorption capacity.

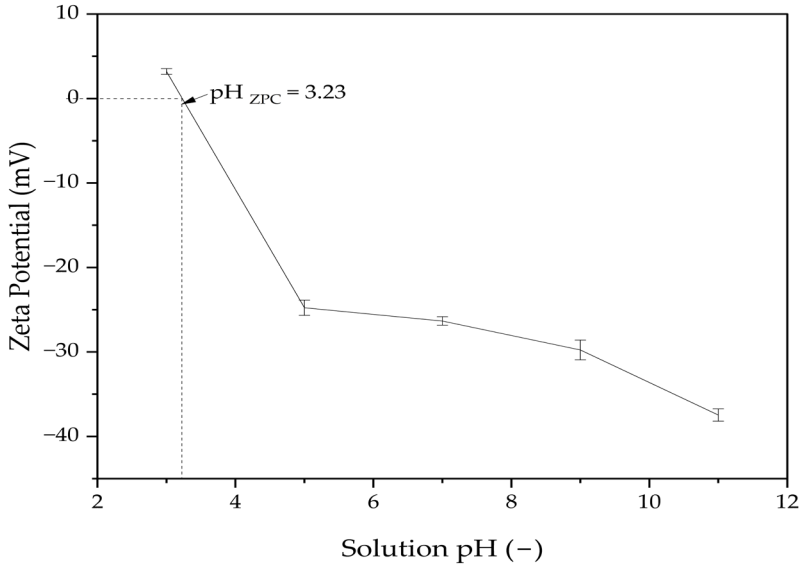

Figure 6. Zeta potential of optimal biochar product (i.e., BC-D-850-I).

4. Conclusions

The anaerobic digestion (AD) process has been widely adopted in the livestock industry for the treatment of animal manure while simultaneously generating biogas for fuel or power. In this study, slurry digestate from the AD process was employed as a novel precursor for the production of porous biochar materials through pyrolysis at tempera-

tures ranging from 550 to 850 °C with a fixed residence time of 30 min. Thermochemical characterization of the dried digestate revealed a high ash content (28.14 wt%), reflecting its complex composition and influencing the pore development of the resulting biochar products. The pore characteristics of the digestate-derived biochars generally increased with rising pyrolysis temperature, although the maximal Brunauer–Emmett–Teller (BET) surface area was limited to approximately 200 m^2/g. The biochars exhibited a combination of microporous and mesoporous structures. Energy-dispersive X-ray spectroscopy (EDS) and Fourier-transform infrared (FTIR) spectroscopy confirmed that the biochars retained oxygen-containing surface functional groups after pyrolysis. Zeta potential analysis further indicated that the biochar surface carried a negative charge at pH > 3.2. Overall, the digestate-derived biochar products were characterized by a well-developed porous structure and negatively charged surface, suggesting potential suitability for various agricultural and environmental applications, particularly in processes involving the adsorption of cationic species.

Author Contributions: Conceptualization, W.-T.T.; formal analysis, C.-H.T. and H.M.M.J.; data curation, C.-H.T. and H.M.M.J.; writing—original draft preparation, W.-T.T.; writing—review and editing, W.-T.T. and H.M.M.J.; supervision, W.-T.T. All authors have read and agreed to the published version of the manuscript.

Funding: This research received no external funding.

Data Availability Statement: The original contributions presented in this study are included in the article. Further inquiries can be directed to the corresponding author.

Acknowledgments: Sincere appreciation is expressed to the National Pingtung University of Science and Technology for their assistance in the scanning electron microscopy (SEM).

Conflicts of Interest: The authors declare no conflicts of interest.

References

1. Baştabak, B.; Koçar, G. A review of the biogas digestate in agricultural framework. *J. Mater. Cycles Waste Manag.* **2020**, *22*, 1318–1327. [CrossRef]
2. Slepetiene, A.; Ceseviciene, J.; Amaleviciute-Volunge, K.; Mankeviciene, A.; Parasotas, I.; Skersiene, A.; Jurgutis, L.; Volungevicius, J.; Veteikis, D.; Mockeviciene, I. Solid and liquid phases of anaerobic digestate for sustainable use of agricultural soil. *Sustainability* **2023**, *15*, 1345. [CrossRef]
3. Chojnacka, K.; Moustakas, K. Anaerobic digestate management for carbon neutrality and fertilizer use: A review of current practices and future opportunities. *Biomass Bioenergy* **2024**, *180*, 106991. [CrossRef]
4. Wang, W.; Lee, D.J. Valorization of anaerobic digestion digestate: A prospect review. *Bioresour. Technol.* **2021**, *323*, 124626. [CrossRef] [PubMed]
5. Tayibi, S.; Monlau, F.; Bargaz, A.; Jimenez, R.; Barakat, A. Synergy of anaerobic digestion and pyrolysis processes for sustainable waste management: A critical review and future perspectives. *Renew. Sustain. Energy Rev.* **2021**, *152*, 111603. [CrossRef]
6. Chozhavendhan, S.; Karthigadevi, G.; Bharathiraja, B.; Kumar, R.P.; Abo, L.D.; Prabhu, S.V.; Balachandar, R.; Jayakumar, M. Current and prognostic overview on the strategic exploitation of anaerobic digestion and digestate: A review. *Environ. Res.* **2023**, *216 Pt 2*, 114526. [CrossRef]
7. Karaeva, J.V.; Timofeeva, S.S.; Bashkirov, V.N.; Bulygina, K.S. Thermochemical processing of digestate from biogas plant for recycling dairy manure and biomass. *Biomass Conv. Bioref.* **2023**, *13*, 685–695. [CrossRef]
8. Wang, W.; Chang, J.S.; Lee, D.J. Anaerobic digestate valorization beyond agricultural application: Current status and prospects. *Bioresour. Technol.* **2023**, *373*, 128742. [CrossRef]
9. Abdelfatah-Aldayyat, E.; González-Rojo, S.; Gómez, X. Reviewing digestate thermal valorization: Focusing on the energy demand and the treatment of process water. *Environments* **2024**, *11*, 239. [CrossRef]
10. Wang, Z.; Li, J.; Yan, B.; Zhou, S.; Zhu, X.; Cheng, Z.; Chen, G. Thermochemical processing of digestate derived from anaerobic digestion of lignocellulosic biomass: A review. *Renew. Sustain. Energy Rev.* **2024**, *199*, 114518. [CrossRef]

11. Fu, Z.; Zhao, J.; Guan, D.; Wang, Y.; Xie, J.; Zhang, H.; Sun, Y.; Zhu, J.; Guo, L. A comprehensive review on the preparation of biochar from digestate sources and its application in environmental pollution remediation. *Sci. Total Environ.* **2024**, *912*, 168822. [CrossRef] [PubMed]
12. Mancuso, G.; Habchi, S.; Maraldi, M.; Valenti, F.; El Bari, H. Comprehensive review of technologies for separate digestate treatment and agricultural valorisation within circular and green economy. *Bioresour. Technol.* **2024**, *409*, 131252. [CrossRef] [PubMed]
13. Zbair, M.; Limousy, L.; Drané, M.; Richard, C.; Juge, M.; Aemig, Q.; Trably, E.; Escudié, R.; Peyrelasse, C.; Bennici, S. Integration of Digestate-Derived Biochar into the anaerobic digestion process through circular economic and environmental approaches—A review. *Materials* **2024**, *17*, 3527. [CrossRef] [PubMed]
14. Masebinu, S.O.; Akinlabi, E.T.; Muzenda, E.; Aboyade, A.O. A review of biochar properties and their roles in mitigating challenges with anaerobic digestion. *Renew. Sustain. Energy Rev.* **2019**, *103*, 291–307. [CrossRef]
15. Shao, Z.; Chen, H.; Zhao, Z.; Yang, Z.; Qiu, L.; Guo, X. Combined effects of liquid digestate recirculation and biochar on methane yield, enzyme activity, and microbial community during semi-continuous anaerobic digestion. *Bioresour. Technol.* **2022**, *364*, 128042. [CrossRef]
16. Alghashm, S.; Song, L.; Liu, L.; Ouyang, C.; Zhou, J.L.; Li, X. Improvement of biogas production using biochar from digestate at different pyrolysis temperatures during OFMSW anaerobic digestion. *Sustainability* **2023**, *15*, 11917. [CrossRef]
17. Basinas, P.; Chamrádová, K.; Vosnaki, O.; Rusín, J. Enhancement of biogas generation by utilizing raw and modified with HNO_3 biochar obtained from pyrolysis of biomass and digestate. *Detritus* **2023**, *24*, 28–39. [CrossRef]
18. Manga, M.; Aragón-Briceño, C.; Boutikos, P.; Semiyaga, S.; Olabinjo, O.; Muoghalu, C.C. Biochar and its potential application for the improvement of the anaerobic digestion process: A critical review. *Energies* **2023**, *16*, 4051. [CrossRef]
19. Tariq, M.; Mehmood, A.; Abbas, Y.; Rukh, S.; Shah, F.A.; Hassan, A.; Gurmani, A.R.; Ahmed, Z.; Yun, S. Digestate quality and biogas enhancement with laterite mineral and biochar: Performance and mechanism in anaerobic digestion. *Renew. Energy* **2024**, *220*, 119703. [CrossRef]
20. Silva, I.; Lapa, N.; Ribeiro, H.; Duarte, E. Pig slurry anaerobic digestion: The role of biochar as an additive towards biogas and digestate improvement. *Appl. Sci.* **2025**, *15*, 1037. [CrossRef]
21. Yang, Q.; Liu, H.; Liu, L.; Yan, Z.; Chui, C.; Yang, N.; Wang, C.; Shen, G.; Chen, Q. Enhancing methane production in anaerobic digestion of food waste using co-pyrolysis biochar derived from digestate and rice Straw. *Molecules* **2025**, *30*, 1766. [CrossRef] [PubMed]
22. Qiao, Y.; Zhang, S.; Quan, C.; Gao, N.; Johnston, C.; Wu, C. One-pot synthesis of digestate-derived biochar for carbon dioxide capture. *Fuel* **2020**, *279*, 118525. [CrossRef]
23. Wang, Y.; Song, Y.; Li, N.; Liu, W.; Yan, B.; Yu, Y.; Liang, L.; Chen, G.; Hou, L.; Wang, S. Tunable active sites on biogas digestate derived biochar for sulfanilamide degradation by peroxymonosulfate activation. *J. Hazard. Mater.* **2022**, *421*, 126794. [CrossRef] [PubMed]
24. Basinas, P.; Rusín, J.; Chamrádová, K.; Kaldis, S.P. Pyrolysis of the anaerobic digestion solid by-product: Characterization of digestate decomposition and screening of the biochar use as soil amendment and as additive in anaerobic digestion. *Energy Convers. Manag.* **2023**, *277*, 116658. [CrossRef]
25. Zheng, X.; Zhang, D.; Wang, F.; Yang, X.; Wang, X.; Chou, S.; Xu, P.; Yi, W. Comparison study on silicon forms and leaching characteristics of pyrolysis biochar and hydrochar derived from cow dung digestate. *J. Anal. Appl. Pyrolysis* **2024**, *183*, 106846. [CrossRef]
26. Hung, C.Y.; Tsai, W.T.; Chen, J.W.; Lin, Y.Q.; Chang, Y.M. Characterization of biochar prepared from biogas digestate. *Waste Manag.* **2017**, *66*, 53–60. [CrossRef]
27. Tsai, W.T.; Fang, Y.Y.; Cheng, P.H.; Lin, Y.Q. Characterization of mesoporous biochar produced from biogas digestate implemented in an anaerobic process of large-scale hog farm. *Biomass Conv. Bioref.* **2018**, *8*, 945–951. [CrossRef]
28. Lowell, S.; Shields, J.E.; Thomas, M.A.; Thommes, M. *Characterization of Porous Solids and Powders: Surface Area, Pore Size and Density*; Springer: Dordrecht, the Netherlands, 2006.
29. Basu, P. *Biomass Gasification, Pyrolysis and Torrefaction*, 2nd ed.; Academic Press: London, UK, 2013.
30. Keiluweit, M.; Nico, P.S.; Johnson, M.G.; Kleber, M. Dynamic molecular structure of plant biomass-derived black carbon (Biochar). *Environ. Sci. Technol.* **2010**, *44*, 1247–1253. [CrossRef]
31. Li, L.; Yao, X.; Li, H.; Liu, Z.; Ma, W.; Liang, X. Thermal stability of oxygen-containing functional groups on activated carbon surfaces in a thermal oxidative environment. *J. Chem. Eng. Jpn.* **2004**, *47*, 21–27. [CrossRef]
32. Islam, M.S.; Ang, B.C.; Gharehkhani, S.; Afifi, A.B.M. Adsorption capability of activated carbon synthesized from coconut shell. *Carbon Lett.* **2016**, *20*, 1–9. [CrossRef]
33. Johnston, C.T. Biochar analysis by Fourier-transform infra-red spectroscopy. In *Biochar: A Guide to Analytical Methods*; Singh, B., Camps-Arbestain, M., Lehmann, J., Eds.; CRC Press: Boca Raton, FL, USA, 2017; pp. 199–228.

34. Qiu, C.; Jiang, L.; Gao, Y.; Sheng, L. Effects of oxygen-containing functional groups on carbon materials in supercapacitors: A review. *Mater. Des.* **2023**, *230*, 111952. [CrossRef]
35. Chia, C.H.; Downie, A.; Munroe, P. Characteristics of biochar: Physical and structural properties. In *Biochar for Environmental Management: Science, Technology and Implementation*, 2nd ed.; Lehmann, J., Joseph, S., Eds.; Routledge: New York, NY, USA, 2015; pp. 89–109.
36. Gregg, S.J.; Sing, K.S.W. *Adsorption, Surface Area, and Porosity*; Academic Press: London, UK, 1982.
37. Li, Q.; Zhang, X.; Mao, M.; Wang, X.; Shang, J. Carbon content determines the aggregation of biochar colloids from various feedstocks. *Sci. Total Environ.* **2023**, *880*, 163313. [CrossRef] [PubMed]
38. Suzuki, M. *Adsorption Engineering*; Elsevier: Amsterdam, The Netherlands, 1990.
39. Kunhikrishnan, A.; Bibi, I.; Bolan, N.; Seshadri, B.; Choppala, G.; Niazi, N.K.; Kim, W.I.; Ok, Y.S. Biochar for inorganic contaminant management in waste and wastewater. In *Biochar: Production, Characterization, and Applications*; Ok, Y.S., Uchimiya, S.M., Chang, S.X., Bolan, N., Eds.; CRC Press: Boca Raton, FL, USA, 2016; pp. 167–219.
40. Cordova, B.M.; Santa Cruz, J.P.; Ocampo, M.T.V.; Huamani-Palomino, R.G.; Baena- Moncada, A.M. Simultaneous adsorption of a ternary mixture of brilliant green, rhodamine B and methyl orange as artificial wastewater onto biochar from cocoa pod husk waste. Quantification of dyes using the derivative spectrophotometry method. *New J. Chem.* **2020**, *44*, 8303–8316. [CrossRef]
41. Kasera, N.; Kolar, P.; Hall, S.G. Nitrogen-doped biochars as adsorbents for mitigation of heavy metals and organics from water: A review. *Biochar* **2022**, *4*, 17. [CrossRef]
42. Gęca, M.; Khalil, A.M.; Tang, M.; Bhakta, A.K.; Snoussi, Y.; Nowicki, P.; Wiśniewska, M.; Chehimi, M.M. Surface treatment of biochar—Methods, surface analysis and potential applications: A comprehensive review. *Surfaces* **2023**, *6*, 179–213. [CrossRef]

Disclaimer/Publisher's Note: The statements, opinions and data contained in all publications are solely those of the individual author(s) and contributor(s) and not of MDPI and/or the editor(s). MDPI and/or the editor(s) disclaim responsibility for any injury to people or property resulting from any ideas, methods, instructions or products referred to in the content.